An Active Microwave Sensor for Near Field Imaging

A. Mirza, C.H. See, I.M. Danjuma, R. Asif, R.A. Abd-Alhameed, J.M. Noras, R.W. Clarke, P.S. Excell

***Abstract*—Near field imaging using microwaves in medical applications is of great current interest for its capability and accuracy in identifying features of interest, in comparison with other known screening tools. This paper documents microwave imaging experiments on breast cancer detection, using active antenna tuning to obtain matching over a wide bandwidth. A simple phantom consisting of a plastic container with a low dielectric material emulating fatty tissue and a high dielectric constant object emulating a tumor is scanned between 4 to 8 GHz with a UWB microstrip antenna. Measurements indicate that this prototype microwave sensor is a good candidate for such imaging applications.**

***Index Terms* — cancer detection, near field imaging, ultra-wideband, microstrip antenna, microwave imaging**

I. Introduction

BREAST CANCER is the most common non-skin related malignancy and the second most common cause in the world of cancer deaths among women, causing many thousands of deaths every year [1]. Until research finds a way to prevent breast cancer, early detection must be looked upon as the best hope for reducing mortality from this disease.

Fifty years ago, there was no established method for detection of breast cancer at an early stage but advances in technology have very much changed the situation. The use of X-ray imaging for detection of breast cancer was proposed in the early days; however, mammography did not become an acceptable technology until the 1960s. Over the past decade, investment in breast cancer research, including early detection, has increased significantly, with new and improved technologies rapidly emerging.

X-ray mammography has proved to be a most effective tool and plays a major role in early breast cancer detection. Despite providing a high percentage of successful detection compared with other screening tools, X-ray mammography also has its limitations. The uncomfortable breast compression associated with this diagnosis method militates against patients undergoing early stage examination and both false positive and false negative rates have been reported [2-4], which suggests a need for screening alternatives. Exposure to ionizing radiation from X-rays is also a concern.

A.Mirza, R. Asif, R.A. Abd-Alhameed, I.M. Danjuma, J.M. Noras and RW Clarke are in the School of Engineering and Informatics, University of Bradford, BD7 1DP, UK (corresponding author 44-1274-23-4033; fax: 44-1274-23-4525; e-mail: r.a.a.abd@bradford.ac.uk).

C.H. See is with School of Engineering, University of Bolton, Bolton, UK.

P.S. Excell is with Glyndwr University, Wrexham, UK.

Recently, other sensors such as Electrical Impedance Tomography Sensor [5], Isotopically Etched Silicon Microarrays [6], Acoustic Biosensor [7] and SiNW-FET in-Air Biosensors [8] have been proposed for better detection of breast cancer. One alternative under investigation is ultra-wideband (UWB) microwave sensors. Based on the variations in the dielectric properties of tissue, this technique permits non-destructive evaluation of the biological tissue, and creates images related to the electrical properties of the breast tissue. The tissue of a malignant tumor has a high water content and hence dielectric properties which are distinct from those of normal breast tissue, which has a lower water content [9]. As a result, strong scattering takes place when microwaves hit the tissue of a malignant tumor.

Microwave imaging of breast tissue can be categorized into three types; passive, hybrid and active methods [3].

- The passive method is based on differentiating malignant and healthy tissue by sensing the inherently increased temperature of the tumor by means of microwave radiometry [9]. Temperature measurements then map out an image of the inspected region of the breast for further diagnosis and verification.
- The hybrid method combines microwave and ultrasonic sensors to determine the presence of a tumor. A tumor has higher conductivity than the normal tissue, so microwave energy is preferentially absorbed by the tumor, heating and expanding it. Using ultrasonic transducers, the pressure wave created by an expanded tumor can be detected and transformed into an image to locate the tumor [10, 11].
- The active method uses microwave radiation into the breast to detect the presence of a tumor and is the most widely adopted method. There are significant differences between the dielectric properties of normal and malignant tissue which alter the reflected signal response [12-17]. A fully mapped image is generated by controlling and reconstructing the backscattered energy.

In this present work, we propose an active microwave method using surface mounting of microwave sensors for breast cancer detection. Specifically, a microstrip sensor is placed on a finite ground plane to eliminate as far as possible the back-scattered waves in the near field zone and thus to direct most of the radiated power into the breast.

II. ANTENNA DESIGN

The case for active microwave imaging as a diagnostic tool for breast cancer detection has been strengthened in recent years due to its improved tissue characterization capability as compared with existing mammography: several prototypes have been constructed and tested [18-20]. Performance is assessed using test "phantoms", targets which closely emulate the actual dielectric mixture of normal and abnormal cancerous tissues. For a feasibility study, it is sufficient to use a uniform block as the phantom, but more sophisticated electromagnetic models for the tissue-sensor interaction can be built up, for example with a two-layer model to represent the breast. The first layer represents the skin, and the second layer the breast tissue, which extends to a width of 10 cm [21-22]. The electrical properties are summarized in Table 1.

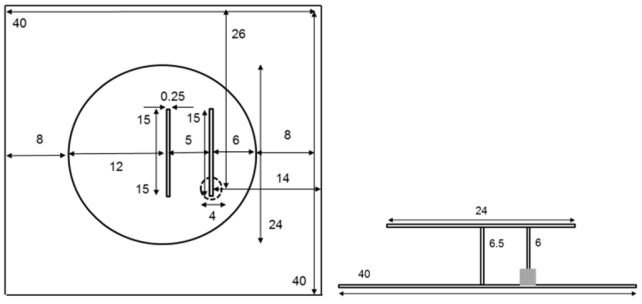

(a)

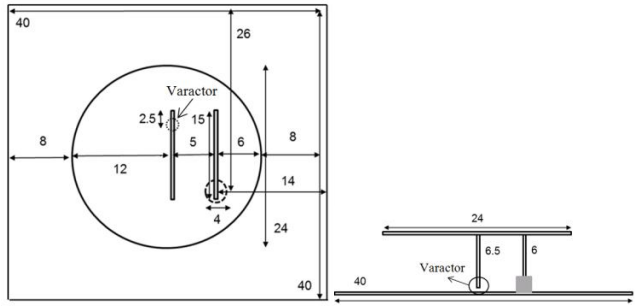

(b)

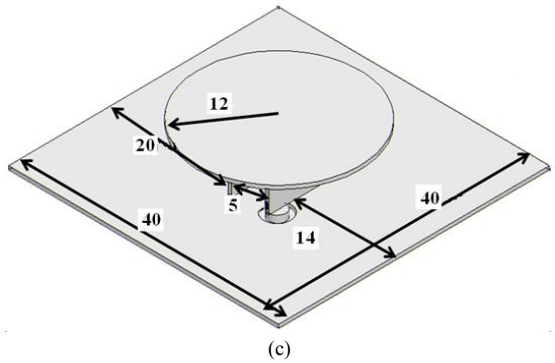

(c)

Fig. 1: Antenna geometry (all units in mm); (a) Proposed antenna, (b) Loaded proposed antenna (c) 3D view

A dual element sensor, for transmission and reception, is investigated in our modelling, and in the subsequent experimental investigations. Mutual coupling between the elements must be taken into consideration within the design and different configurations are investigated through simulation and measurement.

Good electrical matching may be obtained without the addition of a further matching medium or lumped load when the antenna shown in Fig. 1 is in contact with tissue [23-26]. This antenna was fabricated in microstrip, with an air dielectric. The antenna is placed on a ground plane of dimension L= W= 40 mm and thickness 0.5 mm. The antenna is fed via a vertical plate of maximum height 5 mm and a width of 15 mm, which is connected to the feeding probe through an aperture in the ground plane of 4 mm diameter. Another vertical plate with similar dimension was used to short the antenna to the ground as shown in Fig. 1a. The antenna was modelled and optimized using a high frequency structure simulator (HFSS).

TABLE I
BREAST TISSUE ELECTRICAL PROPERTIES

LAYERS	SKIN	BREAST
Thickness / mm	2	100
Relative permittivity	36	9
Equivalent conductivity / Sm^{-1}	4.0	0.4

A parametric simulation was carried out to optimize the performance of the antenna of Fig. 1a before the antenna was manufactured and tested experimentally. Different antenna parameters were considered for optimization of the operating bandwidth, subject to suitable radiated power gain. Relevant parameters include the total size of the ground, feed length, dimensions of the disc, and gap between the vertical plates. To check the influence of these parameters on the impedance bandwidth, in successive tests one parameter was varied while the other parameters remained fixed. Simulation results showed that the effect of changing these antenna dimensions appreciably changed the resonant frequency and return loss. The results can be found in [23], from which the optimum dimensions can be summarized as follows: radius of the circular disc, gap between the vertical plates, ground size and height of the antenna from ground are 12 mm, 5 mm, 40 mm × 40 mm and 5.5 mm respectively. The antenna is designed to be placed directly on the breast so the interaction of the antenna with the tissue was investigated.

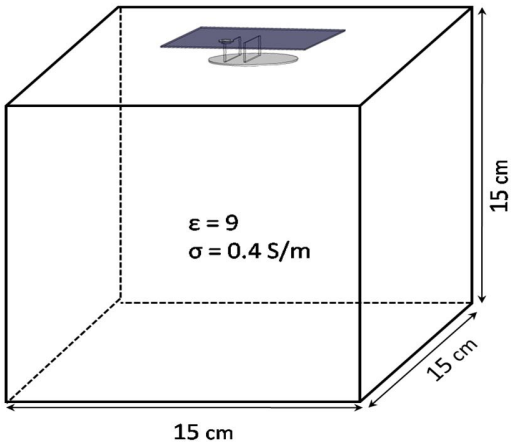

Fig. 2: The geometric model of the antenna with the tissue model

A homogenous block of tissue characterized by conductivity σ = 0.4 S/m and a relative permittivity ε_r = 9 in the form of cubical box of 15 cm side length, has been used as an equivalent model of the interior breast tissue. The antenna geometry including the tissue model is shown in Fig. 2. By observing the resultant reflection coefficient when the antenna is in free space and in contact with the tissue, it is seen that the antenna matching from lower frequencies up to 6.8 GHz was adversely affected by the presence of the tissue. Therefore, the antenna parameters were further optimized with the antenna in contact with the tissue.

After several attempts, good matching was achieved by reducing the height of the antenna from 5.5 mm to 3.5 mm when in contact with the tissue, keeping the remaining dimensions of the antenna fixed. Fig. 3 summarizes the variations of the reflection coefficients of the antenna before optimization with the tissue, after the optimization in free space and in contact with the tissue. As can be seen, the antenna exhibits the required frequency band of interest proposed for this application.

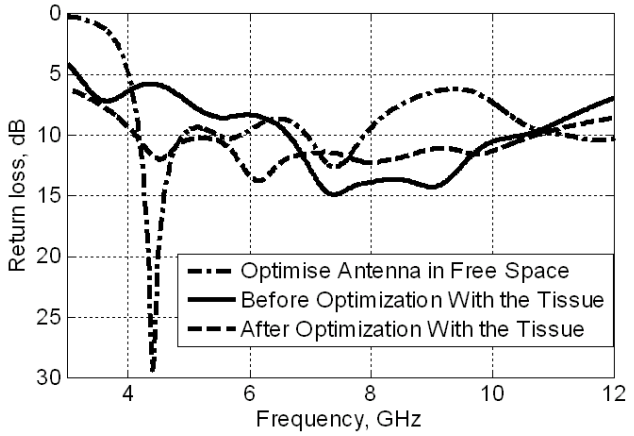

Fig. 3: Antenna input return loss before optimization with the tissue, after optimization in free space and with the tissue.

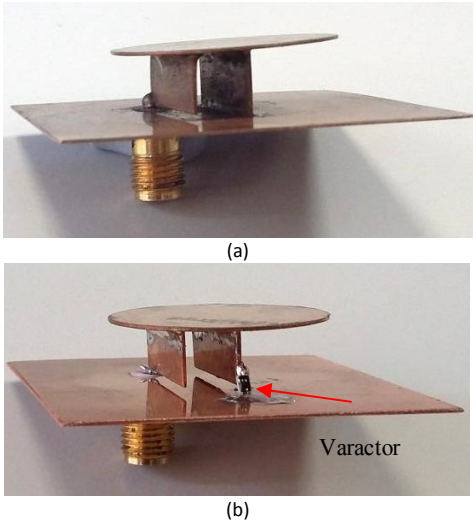

Fig. 4: Physical antenna prototypes (a) without varactor, (b) with varactor.

Two antenna prototypes, i.e. with and without varactor, were fabricated from a copper sheet of thickness 0.25 mm for practical realization, as shown in Fig.4. The GaAs Hyperabrupt Varactor diode, model MGV125-08H20 from Aeroflex was used in the prototype. It has capacitance tunable from 0.1 to 10.5pF over a 1–16 V reverse bias voltage range. A bias tee circuit was integrated at the input port of the antenna. The required decoupling high-Q (>40) capacitor and RF choke inductors were set at 22pF and 1.2nH respectively but are not shown here. An HP 8510C network analyzer was used for measurements. The experimental results in terms of the input return loss of the antenna without the varactor showed reasonable agreement with the results of the simulation, as illustrated in Fig. 5. The impedance bandwidth of the proposed antenna, determined at -10 dB $|S_{11}|$, is 4.4 GHz or about 73.3% with respect to the 6 GHz centre frequency, which fully covers the frequency spectrum required. The slight differences in the return loss curves can be attributed to fabrication inaccuracies.

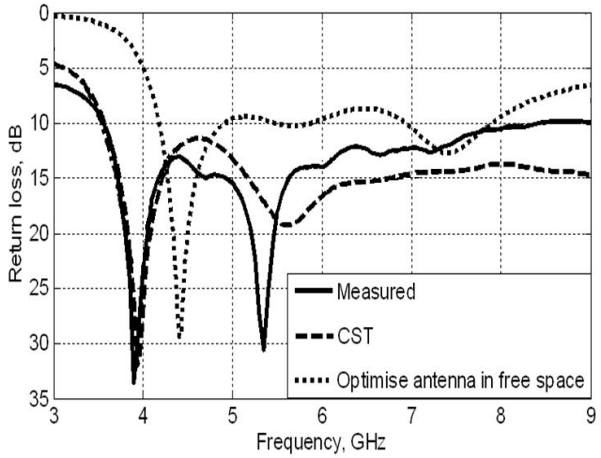

Fig. 5: Measured and simulated input return losses.

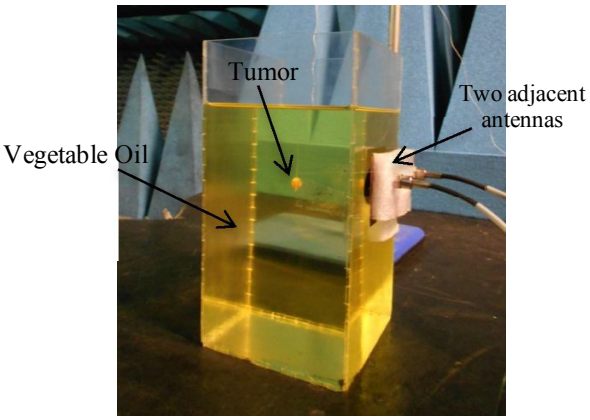

Fig. 6: Experimental set up.

As previously remarked, a breast phantom should ideally closely emulate the actual dielectric mixture of the tissue, and have an equivalent skin barrier. However, a simplified model is used here, to provide basic proof of concept. The approximated breast phantom used for experiments is shown in Fig. 6. It comprises a rectangular tube with dimensions 10.0 cm x 10.0 cm x 20.0 cm, and was initially filled with vegetable oil, the skin being replaced by a Plexiglas barrier of 2 mm thickness. Vegetable oil was used as the dielectric filler

for cost and safety reasons, as has been chosen by others [27-31]. The dielectric constant of the Plexiglas varies from 2.39 to 2.59, with an equivalent conductivity of 0.0093 – 0.007 Sm^{-1} over the range from 3 GHz to 12 GHz [32]: this obviously differs substantially from skin and thus it was decided that skin would be omitted from the proof-of-concept model.

The performance of the pair of antennas was assessed using different locations on the phantom wall to gain physical insight into the relationship between antenna performance and system performance. Three distinct cases were examined as shown in Fig. 7. In case 1, the transmit antenna (TX) and receive antenna (RX) were positioned side by side. In case 2 they are located 90° apart, and 180° apart in case 3.

The analysis began as a simulation exercise, comparing the antenna return loss in air, and adjacent to the oil phantom. Since the final design of the scanner will employ a multiple array around the breast, it is important to investigate the effects of mutual coupling. Initially two identical antennas were analyzed for different separation distances in air, for a range of frequencies. This process was repeated adjacent to the oil phantom. According to a study [33], a coupling level of -20 dB should be used as the target for imaging in the 4 GHz to 8 GHz range.

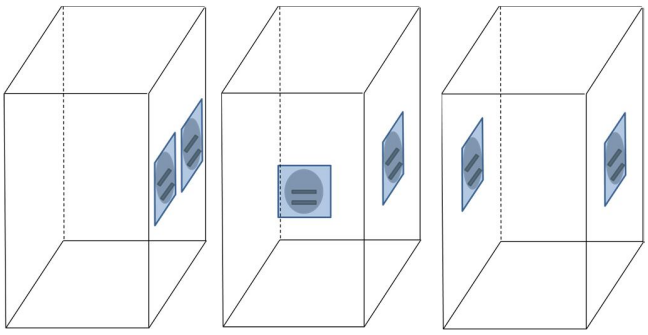

Fig. 7: Investigated locations of the two antennas on the phantom ; (a) case 1 (antennas adjacent), (b) case 2 (antennas 90° apart), (c) case 3 (antennas 180° apart).

III. EXPERIMENTAL SETUP

For experimental verification of the simulation model, S_{11} and S_{21} were monitored for each of the above configurations using a network analyzer, both with the phantom empty and also with it filled with oil. The antennas were in contact with the outer container, and connected to the vector network analyzer (VNA) by coaxial cables.

The scattering material used to represent tumors consisted of 10 g of wheat flour mixed with 5.5 g of water. This mixture has a relative permittivity of 23 and a conductivity of 2.57 S/m at a frequency of 4.7 GHz [34]. It is used to represent tumors of various sizes and placed within the breast phantom oil for experimental detection. In order to compare the performances of the three antenna configurations, several experiments were conducted.

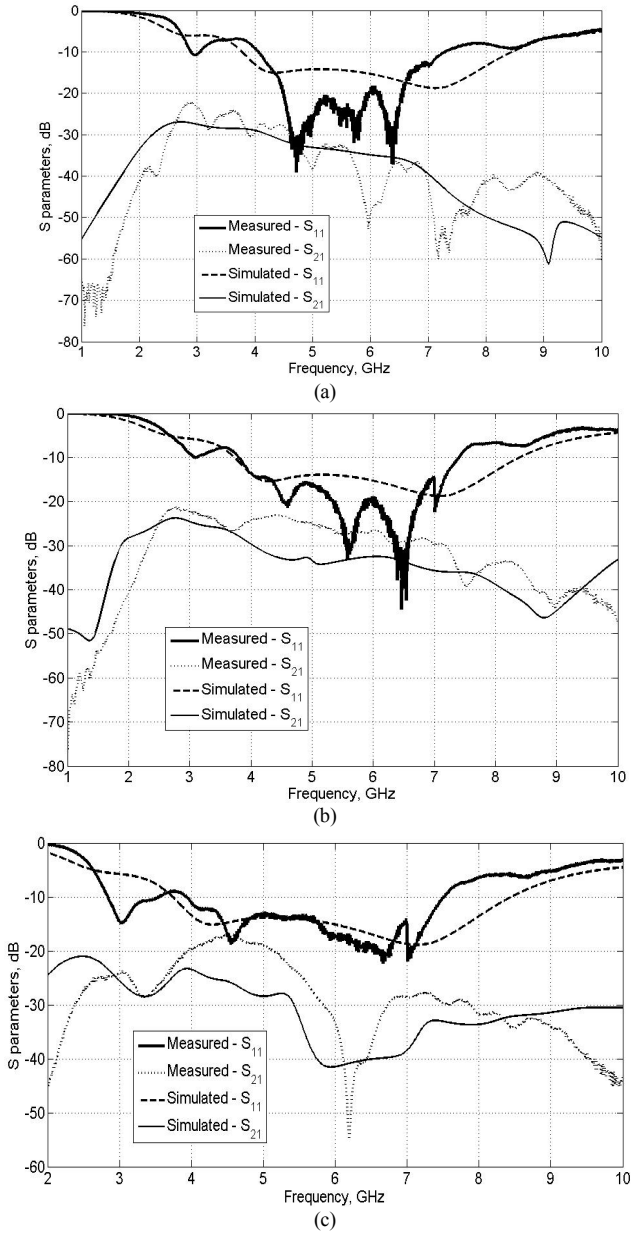

Fig. 8: S_{11} and S_{21} for the antennas with oil-filled phantom; (a) case 1, (b) case 2, (c) case 3 (see Fig. 7).

IV. RESULTS AND DISCUSSIONS

The specific goal here is to measure and analyze the scattered waves due to the transmitted UWB microwave signal travelling through a phantom containing a simulated tumor as described above. In order to evaluate the two-antenna array system we examine S_{11}, S_{21}, the envelope correlation (ρ_e), and the Total Active Reflection Coefficient (TARC). The last two parameters are critical for evaluation of the antenna system; they complement the simple reflection coefficients as they take mutual coupling effects into accounts. They are given by [35]:

$$\rho_e = \frac{\left|S_{11}^{*}S_{12}+S_{21}^{*}S_{22}\right|^2}{\left\{1-\left(\left|S_{11}\right|^2+\left|S_{21}\right|^2\right)\right\}\left\{1-\left(\left|S_{22}\right|^2+\left|S_{12}\right|^2\right)\right\}} \quad (1)$$

$$TARC = \Gamma_a^{'} = \sqrt{\frac{\left|S_{11}+S_{12}e^{j\theta}\right|^2+\left|S_{21}+S_{22}e^{j\theta}\right|^2}{2}} \quad (2)$$

where θ is a random variable with uniform probability density over 0° to 360°.

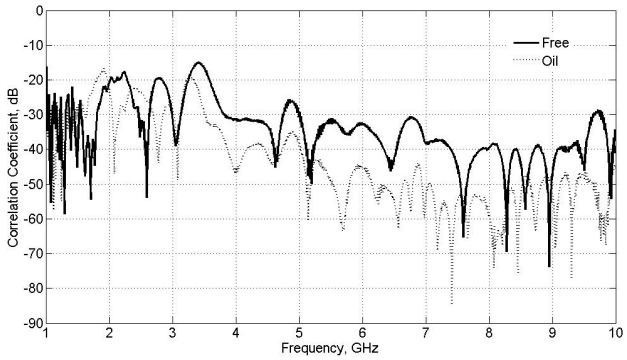

Fig. 9: Measured envelope correlation coefficient for case 1.

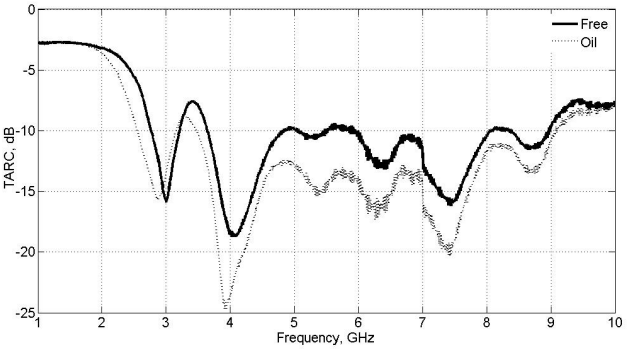

Fig. 10: Measured TARC coefficient for case 1.

The variations of the simulated and the measured scattering parameters for the three test cases shown in Fig. 7 are presented in Fig. 8. These results are obtained with the two antenna elements mounted on the surface of the oil-filled phantom, and show that the antenna array system is working effectively in all three cases over the desired bandwidth, from 4 to 8 GHz. The UWB performance was well confirmed, with the reflection coefficient $|S_{11}|$ < -10 dB over the frequency range, for all test cases. The S_{21} values confirmed the same bandwidth was acceptable for all test cases, ranging between 20 and 30 dB. The S_{21} values are better than the results achieved in our previous work [31] by around 10 dB, because of reduced backscattered radiation achieved here by improved antenna geometry.

The envelope correlation and the TARC for case 1 are shown in Figs 9 and 10, both when the phantom is with and without oil. It is noted that, for the chosen bandwidth, the curves lie below 20 dB and 10 dB respectively for envelope correlation and TARC. The TARC values retain the original behavior of a single antenna, as shown in Fig. 10. However, bandwidth and return loss are changed because TARC is sensitive to the effect of mutual coupling and the phase of the incident wave. Thus, we conclude that the TARC can be interpreted as the return loss of the complete two-antenna array. The results for cases 2 and 3 are quite similar to those for case 1, and thus are not shown here.

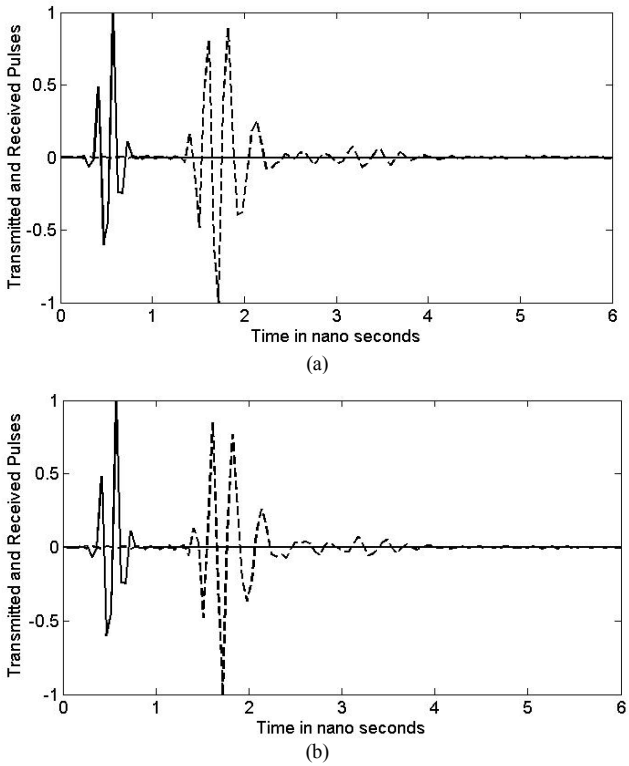

Fig. 11: Measured transmitted and received pulses; (a) with no tumor object, (b) with tumor object.

In one practical example of the case 1 two-element array, a 4 mm tumor was placed at different distances from the antenna plane (10 mm, 15 mm, 30 mm and 40 mm separation) to test sensitivity to reflected signals. The S_{21} transmission parameter was first measured with no scattering object present in the medium and then with the object present. The frequency data was then transferred to reconstruct the time domain pulses with and without the target, as shown in Fig. 11. The normalized back-scattered time responses after subtracting the impressed pulses of these three locations are shown in Fig. 12, showing the sensitivity of the imaging system to this small object: the reflections indicate the magnitude of the signals reflected from the tumor, varying with its depth inside the liquid.

To improve the matching of the antenna with the tissue, a varactor diode was added at the base of the second plate, as shown in Fig. 1b and Fig. 4b. The objective was to achieve active frequency tuning over the total bandwidth with maximum return loss. Fig. 13 shows three tuned frequency spectra with three different varactor capacitances when the antenna was mounted on the second phantom representing a

generic breast as shown in Fig. 14. More values could have been tested, but the values used (0.1, 1 and 5 pF) were found quite adequate to cover the entire intended bandwidth. In the measurement, this three capacitance values are corresponding to 16V, 12.5V and 1.4V applied voltage of the varactor. Both computed and experimental results are in a good agreement.

Collected data were processed with sinusoidal Gaussian pulse shaping to return the reflected magnitude and delay time variations. Several attempts were performed and optimized to reduce the overlap between pairs of these spectra, smoothing the response over ±3 dB of the crossing point.

A single antenna was tested with the phantom structure shown in Fig. 14, but with only one simulated tumor sphere present at two locations 10 mm and 30 mm distant from the skin plane. The normalized reflected magnitude is shown in Fig. 15 and clearly indicates the recovery of the scattered waves in such active operation giving confidence that small antennas in array configurations will be able to detect tumor locations and their expected sizes.

V. IMAGING MODEL SET-UP AND RESULTS

More detailed examples as shown in Figs 14a and b were next investigated to demonstrate the capability of the system. The tissue was of width 50 mm with 2 mm plexiglass containment thickness in both cases. In Fig. 14a three 5mm diameter spheres representing tumors were placed in a plane whose normal distance x_d from the larger face of the container varied between 10 mm and 30 mm with 10 mm steps. In Fig. 14b there are two similar spheres at different distances from the surface: the first is kept fixed at 10 mm while the second was located at variable distances from the surface and 20 mm lower than the first, fixed tumor model. The two-element arrangement of case 1 in Fig. 7a was applied here, with mutual coupling compensated by subtracting the reflection responses without a "tumor" present from those with one or more.

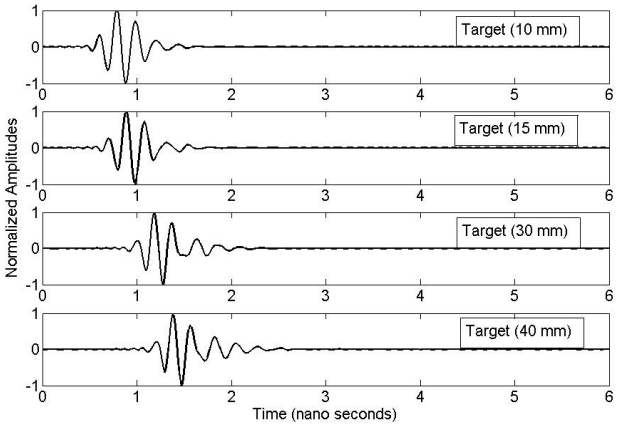

Fig. 12: Comparison of the backscattered responses from various positions.

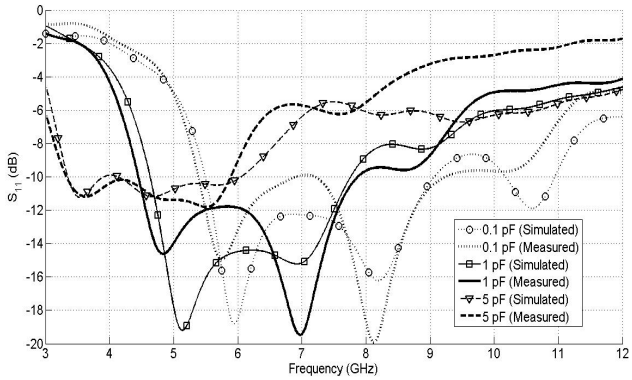

Fig. 13: Simulated and measured S_{11} of the proposed varactor-loaded antenna adjacent to the phantom in Fig. 14, for three values of varactor capacitance.

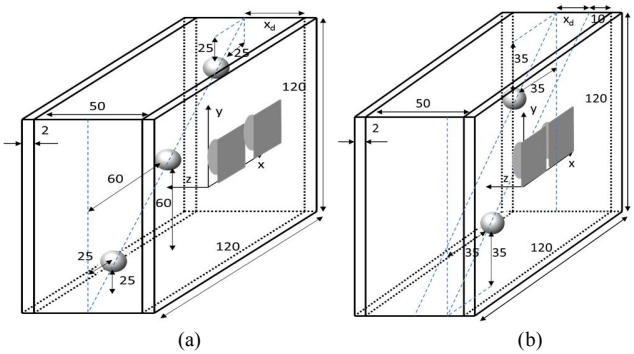

Fig. 14: The tissue model with antenna arrangement including the simulated tumor locations; (a) Three sphere tumor model at the same distances from the skin; (b) Two sphere tumor model: one at 10 mm fixed distance and other at variable distance x_d. (all units in mm).

Fig. 16 shows the magnitude and the time delay of the reflections for the three sphere tumor model of Fig. 14a. In this example the maximum magnitude was normalized to 0dB, and then a dB scale was used in the figures. In the case of the time delay, the values were normalized to 1 nanosecond, and again a logarithmic scale was used. This procedure gives clear images that show the location and the resolution of the tumor plots from these models. The metric of the image performance adopted here is to measure the peak to peak value of the difference in the backscattered reflections with and without the spherical tumor models for each increment move. The corresponding time delay was measured at the absolute maximum of the difference in backscattered reflections. Figs 16: a2, b2 and c2 are extended versions of the magnitudes given in Figs 16: a1, b1 and c1 respectively. The data was interpolated using the piecewise bilinear Gouraud method. The results are encouraging in terms of the feasibility of discriminating and localizing the tumors, at least with a positional resolution of 10 mm or better. The depths of the spheres could be found from Figs 16:a3, b3 and c3. It is clear that even with spheres at 30 mm depth the measurements can yield the approximate distances.

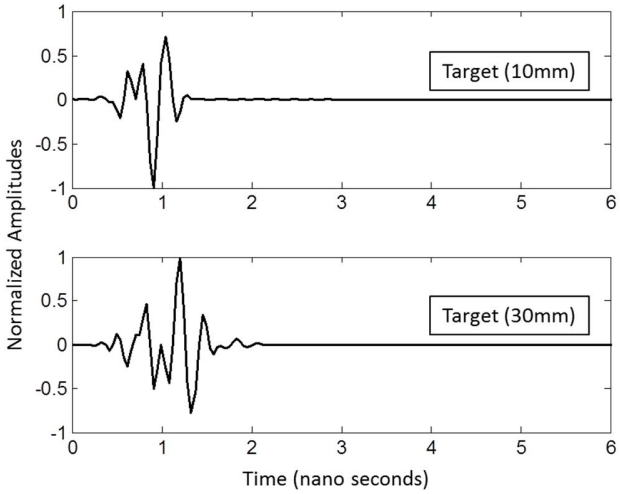

Fig 15: The normalized magnitude of the reflected signal for tumor locations 10 mm (upper trace), and 30 mm (lower trace)

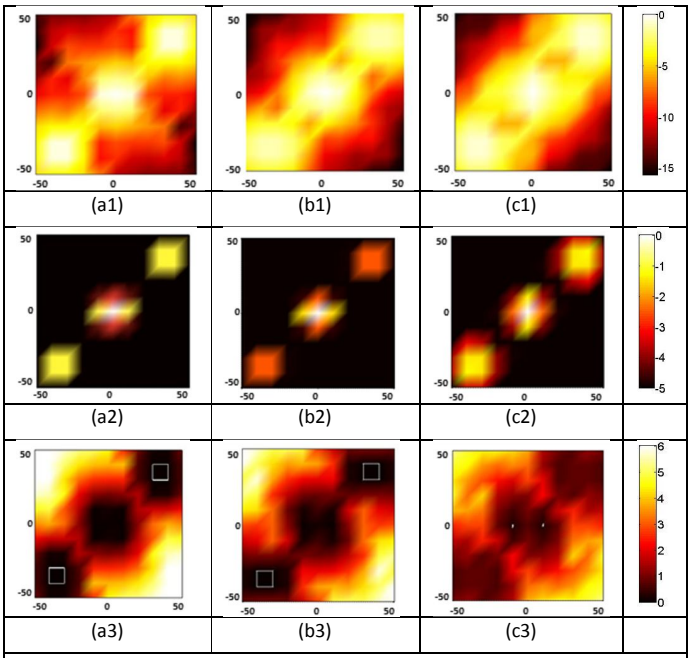

Fig. 16: The magnitude (a1, a2, b1, b2, c1, c2) and the time delay (a3, b3, c3) of the reflected signals for the case in Figure 14a, for various distances x_d; 10 mm (a1, b1, c1), 20 mm (a2, b2, c2), 30 mm (a3, b3, c3)

Fig. 17 also shows the similar analysis as discussed for Fig. 16, but with the setup shown in Fig. 14b. Contour plots have been added to justify the correct locations of the spherical tumor models since the magnitude data was normalized once subject to the total reflections. The magnitude contour plots shown in Figs 17: a2 and a4 clearly identify the locations of both spheres. In addition the time contour plots were also used as evidence of the depths of cancer models. These contour plots were generated subject to the code provided by R. Pawlowicz [36] that handles parametric surfaces with inline contour labels.

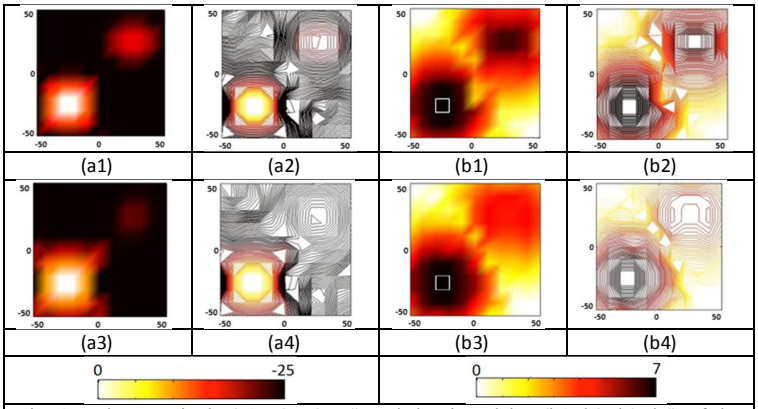

Fig. 17: The magnitude (a1, a2, a3, a4) and the time delay (b1, b2, b3, b4) of the reflected signals of Figure 14b for two distances of x_d; 10 mm (a1, a2, b1 ,b2), 20 mm (a3, a4, b3, b4).

VI. CONCLUSIONS

An experimental investigation was made using small UWB antennas, a breast phantom and simulated tumor targets, and a VNA. The measurements demonstrate that this system is capable of detecting small targets with dimensions comparable to those required for the early detection of breast cancer. Irregularly shaped objects were not tested: however it is anticipated that scattering from such objects will be more pronounced than from a spherical target. A lower limit on size was not determined, but the contrast in the images for 10 mm diameter targets shows that it is likely that smaller target sizes may be detectable under the conditions described in this paper. This confirms the basic design concept, and the choice of antenna elements. The proof of the concept of applying active frequency tuning of the antennas using a varactor diode in order to improve matching performance over the total bandwidth has been demonstrated.

The measurements and the imaging techniques presented in this paper can be used as the basis for investigating a 3D inversion algorithm approach, and further experimental investigation of the super-resolution concept.

ACKNOWLEDGMENT

This work was supported partially from Yorkshire Innovation Fund, Research Development Project (RDP) and Research Council through grant application EP/E022936/1, United Kingdom.

REFERENCES

[1] R.G. Blanks, S.M. Moss, C.E, McGahan, M.J. Quinn, P.J. Babb, "Effect of NHS breast screening programme on mortality from breast cancer in England and Wales, 1990-8: comparison of observed with predicted mortality," pp. 665-669, 2000.

[2] X. Yun, E. C. Fear, and R. H. Johnston, "Compact antenna for radar-based breast cancer detection," *IEEE Trans. Antenna Propagat,* vol. 53, pp. 2374-2380, Aug. 2005.

[3] E. C. Fear, S. C. Hagness, P. M. Meaney, M. Okoniewsk, and M. A. Stuchly, "Enhancing breast tumor detection with near-field imaging," *IEEE Microwave Magazine,* pp. 48-56, March 2002.

[4] S.P. Singh, S. Urooj, A.Lay-Ekuakille, "Breast Cancer Detection Using PCPCET and ADEWNN: A Geometric Invariant Approach to Medical

X-Ray Image Sensors, *IEEE Sensors Journal*, Vol.16, no.12, pp.4847-4855, 2016.
[5] Y.Yang, J. Jia, S.mith, N. Jamil, W. Gamal, P-O Bagnaninchi, "A Miniature Electrical Impedance Tomography Sensor and 3-D Image Reconstruction for Cell Imaging," *IEEE Sensors Journal*, Vol.17, no.2, pp.514-523, 2017.
[6] M. Nikkah, J.S. Strobl, V. Srinivasaraghavan, M. Agah, "Isotopically Etched Silicon Microarrays for Rapid Breast Cancer Cell Capture", *IEEE Sensors Journal*, Vol.13, no.3, pp.1125-1132, 2013.
[7] F.J. Gruhl, K. Lange, "Influence of Surface Preparation Parameters on the Signal Response of an Acoustic Biosensor for the Detection of a Breast Cancer Marker", *IEEE Sensors Journal*, Vol.12, no.6, pp.1647-1648, 2012.
[8] F.Puppo, M-A. Doucey, J-F. Delaloye, T.S. Y. Moh, G. Pandraud, P.M. Sarro, G. D. Micheli, S. Carrara, " SiNW-FET in-Air Biosensors for High Sensitive and Specific Detection in Breast Tumor Extract," *IEEE Sensors Journal*, Vol.16, no.10, pp.3374-3381, 2016.
[9] B. Bocquest, J. C. v. d. Velde, A. Mamouni, G. G. Y. Leroy, J. Delannoy, and D. D. Valee, "Microwave radiometric imaging at 3 GHz for the exploration of breast tumors," *IEEE Trans. Microwave Theory Tech,* pp. 791-793, 1990.
[10] G. Ku , L. V. Wang, "Scanning thermoacoustic tomography in biological tissue," *Med. Phys,* vol. 27, pp. 1195-1202, 2000.
[11] E. C. Fear, "Microwave imaging of the breast," *Technology in Cancer Research & Treatment,* vol. 4, pp. 69-82, February 2005
[12] X. Li, S. C. Hagness, "A confocal microwave imaging algorithm for breast cancer detection," *IEEE Microwave Wireless Comp. Lett,* vol. 11, pp. 130-132, March 2001
[13] E. C. Fear, X. Li, S. C. Hagness, and M. A. Stuchly, "Confocal microwave imaging for breast cancer detection: Localization of tumors in three dimensions," *IEEE Trans. Biomed. Eng,* vol. 49, pp. 812-822, Aug. 2002.
[14] E. C. Fear, M. A. Stuchly, "Microwave detection of breast cancer," *IEEE Trans. Microwave Theory Tech,* vol. 48, pp. 1854-1863, Nov. 2000.
[15] D. Gibbins, M. Klemm, I. J. Craddock et al., "A comparison of a wide-slot and a stacked patch antenna for the purpose of breast cancer detection," *IEEE Trans. on Antennas Propagat.*, vol. 58, no. 3, pp. 665-74, 2010.
[16] M. Klemm, J. A. Leendertz, D. Gibbins et al., "Microwave Radar-Based Differential Breast Cancer Imaging: Imaging in Homogeneous Breast Phantoms and Low Contrast Scenarios," *IEEE Trans. on Antennas Propagat.*, vol. 58, no. 7, pp. 2337-2344, 2010.
[17] R. K. Amineh, A. Trehan, and N. K. Nikolova, "TEM horn antenna for ultra-wide band microwave breast imaging," *Prog. Electromag. Research B,* vol. 13, pp. 59-74, 2009.
[18] Dun Li, P. M. Meaney, T. Raynolds, S. Pendergrass, M. Fanning, K. D. Paulsen, "A parallel-detection microwave spectroscopy system for breast imaging," *Review of Scientific Instruments,* vol. 75, pp. 2305 - 2313, 2004.
[19] P. M. Meaney, K. D. Paulsen, A. Hartov, R. K. Crane, "An active microwave imaging system for reconstruction of 2-D electrical property distributions," *IEEE Transactions on Biomedical Engineering,* vol. 42, pp. 1017 -1026, 1995.
[20] P. M. Meaney, M. W. Fanning, Dun Li, S.P. Poplack, K.D. Paulsen, "A clinical prototype of active microwave imaging of the breast," *IEEE Transactions on Microwave Theory and Techniques,* vol. 48, pp. 1841-1853, Nov. 2000.
[21] Sill J.M, Fear E.C, "Tissue sensing adaptive radar for breast cancer detection: study of immersion liquids," *Electronics Letters,* vol. 41, pp. 113 - 115, 2005.
[22] E.C. Fear, M.A. Stuchly, "Confocal microwave imaging for breast tumor detection: comparison of immersion liquids," in Antennas and Propagation Society International Symposium, Boston, MA, USA , pp. 250 - 253, July 2001
[23] S.Adnan, R.A.Abd-Alhameed, H.I.Hraga I.T.E.Elfergani and M.B.Child, "Compact Microstrip Antenna Design for Microwave Imaging," in *Loughborough Antennas & Propagation Conference*, Loughborough, UK, November 2010, pp. 389 – 392.
[24] S. Adnan, R. A. Abd-Alhameed, M. Al Khambashi, Q. Yousuf, R. Asif, C. H. See, P. S. Excell, A. F. Mirza, Microwave Antennas for Near Field Imaging, IEEE MTT-S IMWS-Bio 2014, 8-10 Dec London, UK, Paper number: MPos1-9; pp. 1-3.
[25] *E.* C. Fear, J. Bourqui, C. Curtis et al., "Microwave breast imaging with a monostatic radar-based system: A study of application to patients," *IEEE Trans. on Microwave Theory and Techniques*, vol. 61, no. 5, pp. 2119-2128, 2013.
[26] M. Lazebnik, D. Popovic, L. McCartney et al., "A large-scale study of the ultrawideband microwave dielectric properties of normal, benign and malignant breast tissues obtained from cancer surgeries," *Physics in Medicine and Biology*, vol. 52, no. 20, pp. 6093-115, 2007.
[27] M.E. Bialkowski, Y. Wang, A. Abu Bakar and W. C. Khor, "Novel Image Reconstruction Algorithm for a UWB Cylindrical Microwave Imaging System," Microwave Symposium Digest (MTT?), 2010 IEEE MTT-S International, pp.477-480, May 2010
[28] M. Bialkowski, D. Ireland , Y. Wang, and A. Abbosh, "Ultra-Wideband Array Antenna System for Breast Imaging," Microwave Conference Proceedings (APMC), 2010 Asia-Pacific, pp.267-270, Dec. 2010
[29] M. Elsdon, D. Smith, M. Leach, and S. J. Foti, "Experimental Investigation Of Breast Tumor Imaging Using Indirect Microwave Holography," *Microwave And Optical Technology Letters,* vol. 48, pp. 480 - 482, 2006.
[30] M. E. Bialkowski, "Ultra Wideband Microwave System with Novel Image Reconstruction Strategies for Breast Cancer Detection," in *Proceedings of the 40th European Microwave Conference*, Paris, France, 28-30 September 2010.
[31] Dan Zhang, Atsushi Mase, "Ultrashort-Pulse Radar System for Breast Cancer Detection Experiment: Imaging in frequency band," in *CJMW2011 Proceedings*, 2011.
[32] P. M. Meaney, K. D. Paulsen, A. Hartov, RK. Crane, "Microwave imaging of tissue assessment: initial evaluation in multitarget tissue equivalent phantoms," *IEEE Transactions on Biomedical Engineering,* vol. 43, pp. 878 - 890, 1996.
[33] H. M. Jafari, J. M. Deen, S. Hranilovic, and N. K. Nikolova, "Co-polarised and cross-polarised antenna arrays for breast, cancer detection," *IET Microw. Antennas Propag,* vol. 1, pp. 1055-1058, 2007.
[34] S. A. Alshehri, S. Khatun, A. B. Jantan, R. S. A. Raja Abdullah, R. Mahmood and Z. Awang, "Experimental Breast Tumor Detection Using Nn-Based Uwb Imaging", *Progress In Electromagnetics Research Symposium (PIERS),* vol. 111, pp. 447 - 465, 2011.
[35] S. H. Chae, S.-K. Oh and S.-O. Park, "Analysis of mutual coupling, correlations, and TARC in WiBro MIMO array antenna," *IEEE Antennas and Wireless Propagation Letters*, Vol. 6, 122–125, 2007.
[36] R.Pawlwlowicz, Contourz function, MATLAB, Available: http://uk.mathworks.com/matlabcentral/fileexchange/3500-contourz/content/contourz.m

Ahmed Faraz Mirza was born in Jhelum, Pakistan in 1987. He re-ceived his

B.Sc. degree in Electrical Engineering from University of Engineering & Technology Lahore Pakistan in 2010, he was awarded M.Sc. degree in Electrical & Electronics Engineering from University of Bradford in 2012. He worked for 2 years as a Field Engineer in a Scotland based packaging company. Currently he is a Ph.D. student and employed as a Research Fellow at the University of Bradford. His research interests include Electromagnetics and Microwave propagation.

Chan See (M'10, S'15) received a first class B.Eng. Honours degree in Electronic,Telecommunication and Computer Engineering and a Ph.D. degree from the University of Bradford, UK in 2002 and 2007 respectively. He is a Senior Lecturer (Programme Leader) in Electrical & Electronic Engineering, School of Engineering, University of Bolton, UK. Previously, he was a Senior Research Fellow in the Antennas and Applied Electromagnetics Research Group within the University of Bradford. He has published over 150 peer-reviewed journal articles and conference papers. He is a co-author for one book and three book chapters. He was a recipient of two Young Scientist Awards from the International Union of Radio Science (URSI) and Asia-Pacific Radio Science Conference (AP-RASC) in 2008 and 2010 respectively. See is a Chartered Engineer, Member of the Institution of Engineering and Technology (MIET) and Senior Member of the Institute of Electronics and Electrical Engineers (SMIEEE). He is also a Fellow of The Higher Education Academy (FHEA).

Isah Musa Danjuma (M'15) was born in Katsina, Nigeria. He received Bachelor of Engineering in Electrical Engineering from Bayero University Kano, Nigeria in 2001 and Master of Technology in Electronic and Telecommunication Engineering from Obafemi Awolowo University Ile-Ife in 2007. Isah is a research student in the Antennas and applied electromagnetics research group within the Electronics, Communications and Information Systems Engineering (ECISE), University of Bradford since February 2016. He is currently working toward his PhD degree. His research focus includes Antenna, Ultra-wideband antennas and Ultra-wideband Radar. Mr Isah is a member of the Institution of Engineering and Technology.

Rameez Asif (M'11) was born in Lahore, Pakistan. He received the B.Eng. degree in electronics and computer engineering from the University of Delaware, Newark, DE., U.S.A. in 2010 and M.Sc. (With Distinction) in electrical and electronics engineering from the University of Bradford, West Yorkshire, U.K., in 2012. He has been a research student in the Antennas and Applied Electromagnetics research group within the Electronics, Communications and Information Systems Engineering (ECISE), University of Bradford since 2012. He is currently working toward the Ph. D degree. He contributed to several international journal articles and conference papers. His research focus includes Antennas, MIMO, Wavelets, and Defected ground antennas. Mr. Rameez has been a member of the Institution of Engineering and Technology.

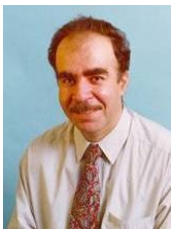

Raed Abd-Alhameed (M'02, S'12) is Professor of Electromagnetic and Radio Frequency Engineering at the University of Bradford, UK. He has long years' research experience in the areas of Radio Frequency, Signal Processing, propagations, antennas and electromagnetic computational techniques, and has published over 500 academic journal and conference papers; in addition he is co-authors of three books and several book chapters. At the present he is the leader of Radio Frequency, Propagation, sensor design and Signal Processing; in addition to leading the Communications research group for years within the School of Engineering and Informatics, Bradford University, UK. He is Principal Investigator for several funded applications to EPSRCs and leader of several successful knowledge Transfer Programmes such as with Arris (previously known as Pace plc), Yorkshire Water plc, Harvard Engineering plc, IETG ltd, Seven Technologies Group, Emkay ltd, and Two World ltd. He has also been a co-investigator in several funded research projects including: 1) H2020 MARIE Skłodowska-CURIE ACTIONS: Innovative Training Networks (ITN) "Secure Network Coding for Next Generation Mobile Small Cells 5G-US", 2) Nonlinear and demodulation mechanisms in biological tissue (Dept. of Health, Mobile Telecommunications & Health Research Programme and 3) Assessment of the Potential Direct Effects of Cellular Phones on the Nervous System (EU: collaboration with 6 other major research organizations across Europe). He was awarded the business Innovation Award for his successful KTP with Pace and Datong companies on the design and implementation of MIMO sensor systems and antenna array design for service localizations. He is the chair of several successful workshops on Energy Efficient and Reconfigurable Transceivers (EERT): Approach towards Energy Conservation and CO2 Reduction that addresses the biggest challenges for the future wireless systems. He has also appointed as guest editor for the IET Science, Measurements and Technology Journal since 2009, and 2012. He is also a research visitor for Wrexham University, Wales since Sept 2009 covering the wireless and communications research areas. His interest in computational methods and optimizations, wireless and Mobile communications, sensor design, EMC, beam steering antennas, Energy efficient PAs, RF predistorter design applications. He is the Fellow of the Institution of Engineering and Technology, Fellow of Higher Education Academy and a Chartered Engineer.

James Noras is a Senior Lecturer in the School of Engineering and Informatics at the University of Bradford, UK, and has published 59 journal and 93 conference papers, in fundamental semiconductor physics, analogue and digital circuit design, digital signal processing and RF system design and evaluation. He is the director of three internationally franchised B.Eng. courses in Electrical and Electronic Engineering. His main research interests are now in digital system design and implementation, DSP and coding for communication systems, and localization algorithms for mobile systems. Dr. Noras is a Member of the Institute of Physics and a Chartered Physicist.

Roger W Clarke (M'06) is a senior lecturer in the Electrical Engineering and Computer Science in the School of Engineering and Informatics at the University of Bradford. Since joining the University in 1987, he has worked on a wide variety of projects in the area of Radio Frequency design within the Antennas, Propagations and RF design research group, Bradford University, UK. Recently, he has worked on multiple-antenna technologies, General electronics for re-configurable antennas, antenna design, battery technology and electric vehicles. His main research interests are Radio frequency, electromagnetic computational techniques, compact sensors design, advanced materials engineering, MIMO systems, energy-efficient and reconfigurable transceivers, beam steering, radio reconfigurable system design and sensors for breast cancer applications. Dr Clarke is member of the Institution of Engineering and Technology and Fellow of Higher Education Academy and a Chartered Engineer.

Peter Excell joined Glyndwr University in 2007, where he is now Deputy Vice-Chancellor. He was previously Associate Dean for Research in the School of Informatics at the University of Bradford, UK, where he had worked since 1971. His long-standing research interests have been in the applications and computation of high-frequency electromagnetic fields. These have led to numerous research grants, contracts and patents in the areas of antennas, electromagnetic hazards, electromagnetic compatibility and field computation. His current work includes studies of advanced methods for electromagnetic field computation, the effect of electromagnetic fields on biological cells, advanced antenna designs for mobile communications, and consideration of usage scenarios for future mobile communications devices. He is a Fellow of the IET, the British Computer Society and the Higher Education Academy, a Chartered Engineer and Chartered IT Professional, a Senior Member of the Institute of Electronics and Electrical Engineers and a member of the Applied Computational Electromagnetics Society.